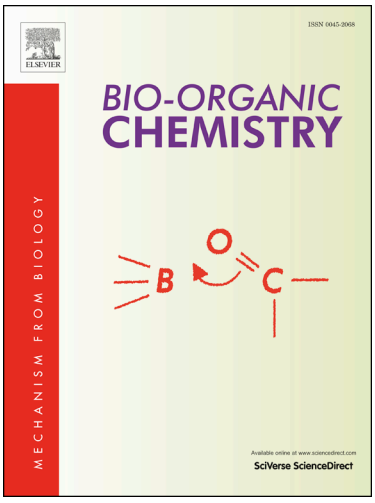

The comparative study of the DNA binding and biological activities of the quaternized dicnq as a dicationic form and its platinum(II) heteroleptic cationic complex

Ufuk Yıldız, Abdurrahman Şengül, Irfan Kandemir, Füsun Cömert, Senem Akkoç, Burak Coban

PII: S0045-2068(18)31394-4
DOI: https://doi.org/10.1016/j.bioorg.2019.03.009
Reference: YBIOO 2835

To appear in: *Bioorganic Chemistry*

Received Date: 30 November 2018
Revised Date: 1 March 2019
Accepted Date: 4 March 2019

Please cite this article as: U. Yıldız, A. Şengül, I. Kandemir, F. Cömert, S. Akkoç, B. Coban, The comparative study of the DNA binding and biological activities of the quaternized dicnq as a dicationic form and its platinum(II) heteroleptic cationic complex, *Bioorganic Chemistry* (2019), doi: https://doi.org/10.1016/j.bioorg.2019.03.009

The comparative study of the DNA binding and biological activities of the quaternized dicnq as a dicationic form and its platinum(II) heteroleptic cationic complex

Ufuk Yıldız[1], Abdurrahman Şengül[1], Irfan Kandemir[2], Füsun Cömert[3], Senem Akkoç[4], Burak Coban[*1]

[*1]Department of Chemistry, Faculty of Arts and Sciences, Zonguldak Bulent Ecevit University, Zonguldak 67100, Turkey

[2]Department of Biology, Faculty of Science, Ankara University, Ankara 06560, Turkey

[3]Department of Microbiology, Faculty of Medicine, Zonguldak Bulent Ecevit University, Zonguldak 67600, Turkey

[4]Faculty of Pharmacy, Suleyman Demirel University, Isparta 32260, Turkey

*Corresponding Author: e-mail: burakcoban@yahoo.com

The comparative study of the DNA binding and biological activities of the quaternized dicnq as a dicationic form and its platinum(II) heteroleptic cationic complex [Pt(bpy)(dicnq)]$(NO_3)_2$

Abstract

The square-planar heteroleptic Pt(II) coordination compound [Pt(bpy)(dicnq)]$(NO_3)_2$ (**1**) and the quaternized dicnq ligand, namely 12,13-dicyano-5,6-dihydrodipyrazino[2,3-*f*:1',2',3',4'-*lmn*][1,10]phenanthroline-4,7-diium dibromide (**2**) (Figure 1) were synthesized and fully characterized by means of FTIR, NMR, MALDI-TOF MS and the purity was confirmed by CHN analyses. The DNA binding profiles of **1** and **2** were identified in an identical condition. The biological activities of these compounds were investigated by the assays of transcription and replication inhibition, cytotoxic and antimicrobial activity.

The result of this study indicates that, both compounds strongly bind to DNA via intercalation but only **1** has a strong nuclease activity. The coordination compound of dicnq (**1**) binds to the DNA only slightly stronger than the quaternized form of dicnq (**2**), and is more potent as an inhibitor of transcription and replication and therefore, **1** has more potential as an anticancer agent but the compounds did not show cytotoxic activity against MCF-7 and MDA-MB-231 breast cancer, and DLD-1 colon cancer cell lines it was found that they only had activities against HepG2 liver cancer cell line with following IC_{50} values; 94.75 and 159.60 µM for **1** and **2**, respectively. In addition, tested bacteria are more susceptible to compound **1**. These biological activities of **1** may strongly be due to its ability to digest DNA as a chemical nuclease. According to this study, the quaternization of the ligand does not make biologically more active than the coordination compound of the same ligand in this case. The compound (**1**) is worth further investigation for its antitumor activities.

Keywords: DNA binding, intercalation, dicnq, transcription inhibition, PCR inhibition, cytotoxicity, antibacterial susceptibility.

Introduction

Cellular DNA is the major target of most antitumor and antibacterial drugs. Therefore, the study of the binding of a small molecule to DNA has been a very attractive field of research in recent years. It is extremely important to determine the binding mode of these molecules for the design of new and more selective DNA-targeted drugs. Molecules can bind to DNA as intercalators, groove binders and electrostatically external binders. After the success of cisplatin, many platinum complexes have been synthesized to study their DNA interactions. On the other hand, cationic nitrogen containing polycyclic aromatic compounds have been known as DNA intercalators such as natural plant alkaloids or synthetic compounds showing antitumor and antibacterial activities (*1*, *2*). A variety of transition metal complexes of a known phenanthroline based ligand, dipyridophenazine (dppz) (*3*, *4*) and one of its important derivatives, 6,7-dicyanodipyrido[2,2-*d*:2′,3′-*f*]quinoxaline (dicnq) have been extensively studied including the crystal structures of Cu(II) and Ag(I) complexes (*5*), spectroscopic properties of Au(III) and Pt(II) complexes (*6*), DNA affinities of Ru(II), Co(II), Ni(II), Mn(II) complexes (*7-11*). In the search for new potential DNA binders, a new square-planar Pt(II) coordination compound $[Pt(bpy)(dicnq)](NO_3)_2$ (**1**) and a new cationic derivative obtained by the quaternization of dicnq ligand, namely 12,13-dicyano-5,6-dihydrodipyrazino[2,3-*f*:1′,2′,3′,4′-*lmn*][1,10]phenanthroline-4,7-diium dibromide (**2**) (Figure 1) have been synthesized, characterized, their DNA binding profiles were identified and finally biological activities including inhibition of transcription and replication, cytotoxicity against MCF-5 and MDA-MB-231 breast, HepG2 liver and DLD-1 colon cancer cell lines and antimicrobial activities against selected bacteria were investigated.

Material and Methods

The synthesis of 6,7-dicyanodipyrido[2,2-*d*:2′,3′-*f*]quinoxaline (dicnq).

An ethanolic solution of 1,10-phenanthroline-5,6-dione (5.0 g, 23.8 mmol) and diaminomaleonitrile (2.57 g, 23.8 mmol) was heated in the presence of a few drops of acetic acid for 2 h under reflux. The mixture was allowed to cool to r.t. and the precipitate was filtered and washed with ethyl alcohol to give an orange-brown solid (3.07 g, 42 %). M.p. 335 °C; FT-IR: 3068 (Ar-CH), 2241 (CN), 1584,

1570, 1505, 1461, 1448, 1387, 1372, 1332, 1262, 1222, 1141, 1074, 1207, 828, 812, 741, 688 cm^{-1}; ^1H NMR (300 MHz, DMSO-d_6) 9.42 (dd, 2H), 9.36 (dd, 2H), 8.05 (dd, 2H); EI-MS m/z 282 (M^+).

Synthesis of Pt(bpy)(dicnq)$(NO_3)_2$ (1).

A solution of dicnq (0.03 g, 0.10 mmol) in ethanol was added into the aqueous solution of [Pt(bpy)$(H_2O)_2$]$(NO_3)_2$ (~0.11 mmol) which was prepared *in situ* (*12*). Then, the mixture was heated under reflux for 2 h. After cooling down to r.t., the solution was diluted with water (60 mL) and then filtered out. To this, a saturated aqueous $NaNO_3$ solution was added at r.t. to allow a yellow precipitate after a few days (0.048 g, 63 %) [Pt(bpy)(dicnq)]$(NO_3)_2$: M.p. 375 °C (decomp.). FT-IR: 3057w (OH), 2240 (CN), 1584vs, 1504vs, 1440vs, 1286vs, 1271vs, 1252vs, 1140vs, 929, 812, 745 cm^{-1}; ^1H NMR: (200 MHz, DMSO-d_6, δ): 9.52 (d, 2H), 9.40 (d, 2H), 8.62 (d, 2H), 8.55 (d, 2H), 8.49 (t, 2H), 8.16 (m, 2H), 7.91 (t, 2H). MALDI-TOF MS *m/z* 758 $[M+H]^+$ (Calculated for $C_{26}H_{14}N_{10}O_6Pt$ 758.08). Calculated for $C_{26}H_{16}N_{10}O_7Pt$ (%): C, 40.27; H, 2.08; N, 18.06. Found (%): C, 40.14; H, 2. 4; N, 17.9.

Synthesis of 12,13-dicyano-5,6-dihydrodipyrazino[2,3-*f*:1′,2′,3′,4′-*lmn*][1,10]-phenanthroline-4,7-diium dibromide (2).

6,7-dicyanodipyridoquinoxaline (dicnq) (0.03 g, 0.1 mmol) in excess of ethylene bromide (5 mL) was heated under reflux for 12 h. The mixture was left to cool down to r.t. and the precipitate was collected by filtration after washing with plenty of acetone and ether to give quarternized dicnq (**2**) (0.014 g, 46%) as gray-green needles: M.p. 380 °C (decomp.). FT-IR: 3432-3376 (OH), 3035 (Ar-CH), 2936 (Alkyl C-H stretch), 2240 (CN), 1587, 1537, 1497, 1414, 1340, 1310, 1242, 1231, 1160, 1110, 1035, 1008, 928, 845, 742, 709 cm^{-1}; ^1H NMR: (300 MHz, $CHCl_3$, δ): 10.3 (d, 2H); 9.79 (d, 2H); 8.81 (dd, 2H); 5.72 (s 4H); ^{13}C NMR: (300 MHz, $CHCl_3$, δ): 156.6, 151.6, 144.0, 137.9, 135.6, 134.4, 133.7, 133.2, 130.1, 128.4, 127.2, 115.7, 53.0. MALDI-TOF MS *m/z* 311.3 [M+H]; calculated for [M+H], 311.10. Anal. Calc. for $C_{18}H_{14}Br_2N_6O_2$: C, 42.71; H, 2.79; N, 16.60 %. Found: C, 42.7; H, 2.9; N, 16.5 %.

Spectroscopic measurements. The absorption spectra were recorded by using Varian Cary 100 spectrophotometer. Perkin Elmer LS 55 fluorescence spectrometer was used to record the emission

spectra. For the measurements, 0.5 mL DMSO solutions of the compounds (about 1 mmol) were prepared and they were diluted to a final concentration of 20 μM by using 5 mM ammonium acetate buffer (pH 7.5) and used for titrations. The CT-DNA stock solution was added in portions of 1 μL and the mixture was incubated for 10 min before the spectra were recorded and repeated until the end of the decrease at the spectrum. The temperature was set to 25 ± 0.1 °C.

The competitive assays for each compound against ethidium bromide (EtBr) were investigated by fluorescence spectrophotometry. The EtBr-DNA complex solution (50:1) was titrated with the compound solutions and the emission peak at 640 nm (ex = 453 nm) was recorded.

Viscosity. The ubbelohde viscometer was used to run the viscosity measurements at a constant temperature of 30.0 ±0.1 °C. The flow times of the DNA solutions (150 μM) in the presence of compounds or DNA alone were measured with a stopwatch with three repeats. Data were presented as $(\eta/\eta_0)^{1/3}$ vs binding ratio, where η is the viscosity of DNA in the presence of the compound and η_0 is the viscosity of DNA alone.

Agarose gel electrophoresis. Plasmid DNA (pBR322) was used in the gel electrophoresis experiments run on 1 % agarose gel in a tris(hydroxymethyl)aminomethane-borate-EDTA (TAE) running buffer solution. The reaction mixtures were prepared (10 mL) in 50 mM ammonium acetate buffer, pH 7.5 at 0 °C containing pBR322 (0.1 μg) and the compounds (0-200 μM) and then incubated at 36 °C for 1 h with and without the addition of 2 μL of 30 % hydrogen peroxide solution. A potential of 35 V for 4 h was applied to the gel at room temperature. The EtBr solution (0.5 μg mL^{-1}) for 30 min was used to stain the gel, soaked in water for 20 min and then visualized under UV light.

Transcription inhibition. RNA synthesis kit and the recommended DNA template from Promega were used for this experiment. The DNA template was incubated with the compounds before it was added to the reaction mixture containing rNTPs (ATP, UTP, CTP, and GTP; 25 mM), T7 transcription buffer, T7 enzyme mix. The mixtures were reacted for 1 h at 37 °C. The products were analyzed by electrophoresis (30 V, 2 h) using 1 % agarose gels and TAE running buffer solution.

Inhibition of PCR amplification. This procedure is a modified method of PCR stop assay carried out in invertebrate (honeybee) mitochondrial DNA (mtDNA) region amplifications (*13*). The PCR inhibition in invertebrate mtDNA was performed through amplification of two mitochondrial gene regions (COI- Carboxyl Oxidase I- approx. 1000bp, CytB-Cytochrome B- approx. 500bp) in honeybee mtDNA separately. The PCR reactions were performed in 1 × PCR mix containing Dream Taq Green PCR Master Mix (Thermo Scientific, #K1082), 10pmol of each primer pairs (COI-F 5′-TTAAGATCCCCAGGATCATG-3′, COI-R 5′-TGCAAATACTGCACCTATTG-3′ and CytB-F 5′-TATGTACTACCATGAGGACAAATATC-3′, CytB-R 5′-ATTACACCTCCTAATTTATTAGGAAT-3′) and the total volume completed to 25 µL with PCR grade pure water. PCR reactions for both honeybee mtDNA regions were incubated in a thermocycler with the following cycling conditions: 94 °C for 1 min, followed by 35 cycles of 94 °C for 1 min, 50 °C for 2 min and 72 °C for 3 min. Amplified PCR products were resolved on 1 % agarose gel, EtBr stained and photographed under UV light.

Cell culture. Human breast epithelial adenocarcinoma cancer cell line (MCF-7), human liver epithelial hepatocellular carcinoma cell line (HepG2), human breast epithelial adenocarcinoma cell line (MDA-MB-231) and human epithelial colorectal adenocarcinoma cell line (DLD-1) were cultured in DMEM medium supplemented with 10% FBS and 1% Glutamax. The cells were seeded into sterile 96-well plates at a density of 4 × 103 cells/well and maintained at 37 °C under a humidified atmosphere containing 5% CO_2 for 24 h. After 24 h and 48 h incubation time, seeding cells were exposed to compounds at nine different concentration following 200, 100, 50, 20, 10, 5, and 5 µM. Then, 96-well plates were again incubated for 24 h. Then, MTT stock solution (50 µL, 5 mg/mL) was added to each well and was incubated in an incubator for 4 h. Then, medium was removed and 200 µL of DMSO was added to each well. The plates were placed on a plate rocker for 30 minutes. The absorbance values were measured at 560 nm using Promega reader device. IC50 values were calculated with the GraphPad Prism 7 software program.

Antimicrobial activity of the compounds was determined by the micro-broth-dilution method, as recommended by the European Committee on Antimicrobial Susceptibility Testing (EUCAST). The

stock solutions were prepared in DMSO at 500 mg/µl and serial two-fold dilutions of each chemical (totally 10 dilutions between 250-0.48 µg/ml) were prepared with the cation-adjusted Mueller-Hinton broth (CAMHB) in sterile 96-well polystyrene U-bottom broth micro-dilution trays. *Staphylococcus aureus* ATCC 29213, *Enterococcus faecalis* ATCC 29212, *Escherichia coli* ATCC 25922 and *Pseudomonas aeruginosa* ATCC 27853 were used (10^4 CFU/well) as test microorganisms. Cefotaxime was used as the control antimicrobial. The lowest concentration of the compounds and antimicrobial demonstrating complete inhibition of growth was determined as minimal inhibitor concentration (MIC). Tests were repeated twice.

Results

Chemistry

The ligand dicnq was synthesized according to the method explained elsewhere (*7, 14*). The product was obtained in good yield. The FTIR and ^{1}H NMR data are identical to the literature data. The characteristic CN stretching appears at around 2240 cm^{-1} in the IR spectra of all compounds. The IR spectra of the cationic derivative **2** and the Pt(II) complex (**1**) show the OH stretching vibrations at around 3400-3600 cm^{-1} due to the presence of lattice water in both molecules. The observed doublet at 3432-3376 cm^{-1} in the spectrum of **2** can be assigned to the hydrogen bonded water molecules in the lattice (*11*). The IR spectrum of **2** shows the characteristic stretching of the aliphatic protons at 2936 cm^{-1} that undoubtedly confirms the attachment of the ethylene group to the tertiary N atoms of the ligand (dicnq) that is an evidence of the completion of the quaternization. The remaining peaks are very similar with only slightly shifting of the corresponding C=N and C=C stretching vibrations as expected. In the ^{1}H NMR, the observed three doublet of doublets at the aromatic region of the ^{1}H NMR spectra confirm the symmetrical 1,10-phenanthroline moiety (*6, 7, 14*). The precursor, $Pt(bpy)Cl_2$ (*13*) was treated with an equimolar amount of $AgNO_3$ in aqueous solution. In order to remove the fine powder of AgCl precipitate, the solution was repeatedly filtered and finally centrifuged. The resulting pale yellow solution of $[Pt(bpy)(H_2O)_2](NO_3)_2$ was treated with dicnq in

ethanol, then the mixture was set to reflux for three hours and finally followed by the addition of a saturated $NaNO_3$ solution to give $[Pt(bpy)(dicnq)](NO_3)_2$ (**1**). The MALDI-TOF MS, the observed molecular mass at *m/z* 757, confirms the purity and the integrity of **1**. The CHN analysis showed that the complex is monohydrated in the solid state as revealed by the IR which shows the characteristic vibration bands between 3200 and 3500 cm^{-1}. In the ^1H NMR spectrum, the aromatic protons (α) (Table 1) adjacent to imine nitrogen were shifted because of the coordinating platinum atom. The additional four peaks belonging to the bipyridine ligand further confirms the structure of the complex.

Dicnq in excess of ethylene bromide was heated at reflux under dry nitrogen atmosphere for 3 hours to yield the quaternized dicnq (**2**) as a bromide salt. In the IR spectrum, the peaks at 2240 and 2931 cm^{-1} which are attributable to the nitrile and the alkyl groups, respectively, support the structure. The protonated nitrogen atoms in **2** caused deshielding of the aromatic protons as listed in Table 1. The aliphatic protons which appear at 5.72 ppm in the ^1H NMR spectrum and the aliphatic carbon atoms at 53 ppm in the ^{13}C NMR spectrum clearly confirm the completion of the quaternization of the 1,10-phenanthroline tertiary N atoms in **2**. The MALDI-TOF MS further confirms the molecular structure at *m/z* 311.3. The CHN analysis confirms that this highly charged compound has two molecules of water of crystallization in the solid state which is well agreed with the FTIR showing a characteristic water stretching band at 3432 cm^{-1}.

Figure 1

Table 1. Comparison of the ^1H NMR chemical shifts of aromatic protons of the dicnq compounds.

Compounds		Protons (ppm)			solvent
		α	***β***	***γ***	
dicnq	[6]	9.38	8.03	9.38	$DMSO\text{-}_{d6}$
dicnq		9.47	7.97	9.52	$CDCl_3$
q-dicnq	(**2**)	9.80	8.80	10.30	$CDCl_3$

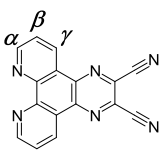

$[Pt(bpy)dicnq]^{2+}$	(**1**)	8.55	8.49	9.52	$DMSO\text{-}_{d6}$

DNA binding studies

UV titration experiment is a valuable method to study the interactions of compounds with DNA. An apparent hypochromism and a bathochromism in the spectrum can be attributed to intercalation mode of binding to DNA. Figure 2 shows the absorption spectra of the compounds in the absence and presence of CT-DNA. With the addition of DNA to **1** or **2**, the apparent hypochromism with 1-2 nm red shift in the UV spectrum was observed. The hypochromism was found to be 18 % for **1** and 14 % for **2** at around 1:1 DNA-to-drug concentration ratio. For a better evaluation and the comparison between two compounds, the binding constants K_b were calculated:

$$[DNA]/(\varepsilon_A-\varepsilon_f)= [DNA]/(\varepsilon_B-\varepsilon_f) + 1/K_b(\varepsilon_B-\varepsilon_f) \quad (1)$$

where [DNA] is in base pairs, ε_A is absorption coefficient of the compound for each measurement, and ε_f and ε_B are absorptivity values of free and the fully bound form of the compound. The binding constant K_b is given by the ratio of the slope to the intercept in the $[DNA]/(\varepsilon_A-\varepsilon_f)$ *vs* [DNA] plot. The calculated binding constants were found 8.2 (± 0.5) and 8.0 (± 0.4) × 10^5 M^{-1}. Both compounds have higher binding affinities against ds-DNA in comparison to the original ligand (*11*). The platinum(II) complex (**1**) binds stronger than the analogous $[Pt(bpy)en]^{2+}$ indicating that the addition of dicnq ligand significantly improves the binding of the complex (*15*) (Table 2). The quaternized dicnq (**2**) can bind to DNA stronger than the free ligand itself (Table 2), probably because of the additional positive charges on the ligand having potential electrostatic interaction ability with the anionic phosphate groups of the DNA structure. In comparison, the octahedral $[Mn(dicnq)(H_2O)_3(NO_3)]^+$ complex ion has a similar binding affinity while 1,10-phenanthroline complexes of Ru(II), Ni(II), Co(III) with dicnq have lower binding values (Table 1) (*7, 10, 11*). This may be due to the steric effect of the two additional phenanthrene rings of these octahedral complexes. The results are also compatible to those of other cationic compounds and the Pt(II) complexes such as q-dppz (K_b= 3.4 × 10^5 M^{-1}), q-pip (K_b= 4.4 × 10^5 M^{-1}), and q-hpip (K_b= 7.5 × 10^5 M^{-1}), $[Pt(bpy)(pip)]^{2+}$ (K_b= 2.9 × 10^4 M^{-1}), $[Pt(bpy)(hpip)]^{2+}$

(K_b= 5.4 × 10^4 M^{-1}), $[Pt(bpy)(iip)]^{2+}$ (K_b= 3.6 × 10^4 M^{-1}), and $[Pt(bpy)(miip)]^{2+}$ (K_b= 7.0 × 10^4 M^{-1}) (*4, 16-19*).

Figure 2

Table 2. A comparison of **1** and **2** with dicnq and its other analogous metal complexes in the literature according to the binding parameters by the UV titration method.

Compounds	References	UV-max. (nm)	K_b (×10^4 M^{-1})	Red shift (nm)	Hypochromism (%)
dicnq	[10]	305	17.0	5	18
Pt(dicnq)(bpy) (**1**)	-	310	82.0	1	18
$[q\text{-dicnq}]^{2+}$ (**2**)	-	451	80.0	2	14
$[Mn(dicnq)(H_2O)_2NO_3]^{+}$	[10]	305	50.0	6	24
$[Co(dicnq)(phen)_2]^{3+}$	[9]	409	0.6	3	28
$[Ni(dicnq)(phen)_2]^{2+}$	[9]	369	2.1	5	35
$[Ru(dicnq)(phen)_2]^{2+}$	[6]	351	3.3	4	16
$[Pt(bpy)(en)]^{2+}$	[14]	317	15.6	5	49

Competitive fluorescence studies have been extensively used for the identification of the binding mode based on the competition between the unknown drug and a known fluorescence dye with a known binding mode. This is very useful if a dye with high fluorescence emission at the binding site of DNA reduces its fluorescence intensity when it is subjected to the addition of the unknown drug, this means that both unknown drug and known dye have the same binding mode to DNA. Figure 3 shows the changes in the fluorescence intensity of ethidium bromide (EtBr) a known intercalator (*20*) bonded to DNA with the additions of **1** and **2**. Both compounds reduce the fluorescence intensity of EtBr emission indicating that they bonded to DNA via intercalation or in some cases as groove binders (*21*).

The binding constants can be calculated by the classical Stern–Volmer;

$$I_0/I = 1 + K_{app} \qquad (2)$$

where I_0 and I represent the fluorescence intensities in the absence and presence of a compound; K_{app} is a linear Stern–Volmer quenching constant dependent on the quenching plot of I_0/I vs. [compound]/[DNA] (Figure 3). The binding constant of EtBr was used as 4.5×10^5 M^{-1} (*22*), the calculated DNA binding constants (K_{app}) were 8.8×10^5 and 3.8×10^5 M^{-1} for **1** and **2**, respectively. These binding values well correlate with those of UV–vis titration.

Figure 3

Viscosity measurements are reliable and precise to length change and an indication of a classical intercalation (*23*). Figure 4 shows the effects of EtBr, **1** and **2** on the viscosity of DNA. The classical intercalator, EtBr, increased the viscosity of DNA. A concentration-depended slight viscosity increase compares to EtBr indicates that **1** and **2** are intercalating between the DNA base pairs (*4*).

Figure 4

The gel electrophoresis was used to study DNA cleavage activities of the compounds. Supercoiled plasmid DNA, pBR322 in ammonium acetate buffer (pH 7.5) was used in this study. Plasmid DNA pBR322 in its form I resembles a relatively long run on the gel and cleavage on one strand generates an open circular form (form II) creating a short move on the gel (*24*). Figure 5 shows agarose gel electrophoresis assay of pBR322 incubated with each of compounds. With increasing concentration of **1** (Figure 5A, lane 2-3), the amount of form I of pBR322 diminished gradually. Multiple scissions in the DNA were occurred by **1** and small fragments of DNA cannot be visualized in the gel as indicated by the previous studies (*15, 25, 26*). On the other hand, **2** showed no effect on the DNA structure even at high concentration (Figure 5B). However, in the presence of hydrogen peroxide, single strand DNA cleavage was observed for pBR322 treated with **2**, the form I gradually diminished, while form II

increased. According to these results, **1** exerts extensive damage to the DNA but **2** generates a moderate cleavage on the DNA backbone when an oxidizing agent is used.

Figure 5

Biological activities

Transcription inhibition: A variety of anticancer agents act as inhibitors of DNA transcription(*27-30*). The inhibitors of transcription usually stabilize the double-stranded DNA template by non-covalent binding and therefore prevent the strand separation. Some transition metal complexes of planar polypyridyl ligands were shown to inhibit transcription by the degree of their binding to dsDNA (*31, 32*). Figure 6 shows a varying concentration of the compounds affecting the amount of mRNA produced by transcription. The control lanes indicate the maximum amount of the production with no compounds added. Increasing concentration of both compounds decreased the amount of the mRNA produced in a concentration depended manner (lanes 3–5). The inhibition of transcription was more effective by **1**, when the concentration of both compounds was 400 μM and over (lanes 5-6) transcription was completely inhibited, another word, there is no mRNA synthesized. This result is coherent with the DNA binding studies.

Figure 6

Inhibition of PCR amplification: PCR (Polymerase Chain Reaction) is a revolutionary method developed by Kary Mullis in the 1980s (*33*). PCR is based on using the ability of DNA polymerase to synthesize new strand of DNA complementary to the offered template strand. It is an *in vitro* DNA replication reaction. The compounds **1** and **2** were further evaluated by using a PCR assay if they can

stabilize the DNA duplex template, and therefore inhibit DNA polymerase. Figure 7 shows the PCR final products of the assay mixtures containing compounds. The DNA polymerase inhibition was very effective for inhibiting the enzyme at a low concentration of **1** for the 500 bp long cyt-B template but at higher concentration for the 1000 bp long CO-I template. Whereas, **2** is almost inactive for DNA polymerase even at very high concentrations for both templates.

Figure 7

Cytotoxic activity: Compounds were screened for learning their cytotoxic activity against MCF-7, HepG2, MDA-MB-231 and DLD-1 cell lines using the MTT assay method for a period of 24 h and 48 h. The IC50 results are given in Table 3. In this study, we firstly screened our samples for 24 h against breast cancerous cell line (MCF-7). However, IC_{50} values were obtained higher than 200 µM. Therefore, the screening time was increased from 24 h to 48 h. However, the values obtained were again greater than 200 µM. Likewise; they were also tested in MDA-MB-231, HepG2 and DLD-1 cell lines for 48 h. However, according to above MTT results, compounds **1** and **2** had not efficiency in two mentioned breast cancerous cell lines and colon cancer cell line, it was found that they only had activities in the liver cell line (HepG2) with following IC_{50} values; 94.75 and 159.60 µM for **1** and **2**, respectively. On the other hand, the positive control drugs cisplatin and ploxal-S gave lower IC_{50} values as 30.38 and 22.25 µM, respectively.

Table 3. IC_{50} values of the compounds **1** and **2** against cancerous cell lines.

Compounds	**IC_{50} (µM)**				
	MCF-7		**HepG2**	**MDA-MB-231**	**DLD-1**
	24 h	48 h	48 h	48 h	48 h
1	>200	>200	94.75	>200	>200
2	>200	>200	159.60	>200	>200
Cisplatin	9.72	N.T.*	30.38	2.78	60.79
Ploxal-S	N.T.*	27.60	22.25	4.30	N.T.*

N.T.* Not tested

Figure 8

Antimicrobial activity: Identified MIC values of the compounds are given in Table 4. MIC of the control microorganism (Escherichia coli ATCC 25922) was 0.03 µg/ml for cefotaxime (expected value; 0.03-0.125 µg/ml).

The platinum(II) complex (**1**) showed a moderate antimicrobial activity against all microorganisms tested but **2** has a very weak or no activity. This result is consistent with the nuclease activities of the compounds. A number of platinum(II) complexes have been also shown to have similar antibacterial activities (*34-36*).

Table 4. Identified MIC values of the compounds **1** and **2**.

Compounds	*S. aureus ATCC 29213*	*E. faecalis ATCC 29212*	*E. coli ATCC 25922*	*P. aeruginosa ATCC 27853*
1	31.2	15.6	31.2	31.2
2	125	250	125	125

Conclusions

Two compounds of dicnq: a square-planar heteroleptic Pt(II) coordination compound Pt(bpy)(dicnq)$(NO_3)_2$ (**1**) and a quaternized dicnq 2,13-dicyano-5,6-dihydrodipyrazino[2,3-*f*:1',2',3',4'-*lmn*][1,10]phenanthroline-4,7-diium dibromide (**2**) are reported. A number of physicochemical methods suggested that these compounds strongly bind to DNA via intercalative binding interactions with different binding affinities. The nuclease activities of the compounds against pBR322 DNA indicate that **1** severely digests the nucleic acid in low concentrations. On the other hand, **2** itself is inactive but induces single strand cleavage only in the presence of peroxide. The DNA functions: transcription and replication are inhibited by **1** and therefore it can be considered as a potential antitumor agent, both compounds were found to be moderately active against HepG2 liver cancer cell line and **1** is more active but no activities found against other cell lines tested. On the other hand, **1**

also showed weak antibacterial activities against both gram-positive and gram-negative bacteria whereas **2** showed a very weak or no activity. These biological activities of **1** may be related to the nuclease activities of this compound. Further studies are required to assess the cytotoxic properties of **1** *in vivo* against different cell lines to elucidate the actual mechanism of its biological activity.

Acknowledgements

We are grateful for the financial support of Zonguldak Bulent Ecevit University with grant # 2015-72118496-13. We thank to Ms. Tuğba Demiray and Ms. Sena (Apaydın) Hasanoğlu for the technical contribution to the project.

References

[1]. T.P. Cushnie, B. Cushnie, and A.J. Lamb, Alkaloids: an overview of their antibacterial, antibiotic-enhancing and antivirulence activities, Int. J. Antimicrob. Agents. 44 (2014) 377-386. https://doi.org/10.1016/j.ijantimicag.2014.06.001.

[2]. Z. Habli, G. Toumieh, M. Fatfat, O.N. Rahal, and H. Gali-Muhtasib, Emerging Cytotoxic Alkaloids in the Battle against Cancer: Overview of Molecular Mechanisms, Molecules. 22 (2017). https://doi.org/10.3390/molecules22020250.

[3]. A.E. Friedman, J.C. Chambron, J.P. Sauvage, N.J. Turro, and J.K. Barton, A molecular light switch for DNA: Ru(bpy)2(dppz)2+, J. Am. Chem. Soc. 112 (1990) 4960-4962. https://doi.org/10.1021/ja00168a052.

[4]. T. Phillips, I. Haq, A.J.H.M. Meijer, H. Adams, I. Soutar, L. Swanson, M.J. Sykes, and J.A. Thomas, DNA Binding of an Organic dppz-Based Intercalator, Biochem. 43 (2004) 13657-13665. https://doi.org/10.1021/bi049146r.

[5]. M.D. Stephenson, and M.J. Hardie, Extended Structures of Transition Metal Complexes of 6,7-Dicyanodipyridoquinoxaline: π-Stacking, Weak Hydrogen Bonding, and CN·π Interactions, Crystal Growth & Design. 6 (2006) 423-432. https://doi.org/10.1021/cg050366t.

[6]. K.P. Balashev, M.A. Ivanov, T.V. Taraskina, and E.A. Cherezova, Spectroscopic and electrochemical properties of mixed-ligand cycloplatinated complexes based on 2-(2-thienyl)pyridine and 2-phenylpyridine with 1,10-phenantroline and its 1,4-diazine derivatives, Russian J. Gen. Chem. 76 (2006) 781-790. https://doi.org/10.1134/s1070363206050215.

[7]. A. Ambroise, and B.G. Maiya, Ruthenium(II) Complexes of 6,7-Dicyanodipyridoquinoxaline: Synthesis, Luminescence Studies, and DNA Interaction, Inorg. Chem. 39 (2000) 4264-4272. https://doi.org/10.1021/ic9914692.

[8]. S. Arounaguiri, and B.G. Maiya, "Electro-Photo Switch" and "Molecular Light Switch" Devices Based on Ruthenium(II) Complexes of Modified Dipyridophenazine Ligands: Modulation of the Photochemical Function through Ligand Design, Inorg. Chem. 38 (1999) 842-843. https://doi.org/10.1021/ic981109z.

[9]. X. Chen, F. Gao, W.-Y. Yang, J. Sun, Z.-X. Zhou, and L.-N. Ji, Effects of intercalative ligands on the DNA binding, DNA topoisomerase II and DNA transcription inhibition of polypyridyl ruthenium(II) complexes, Inorg. Chim. Acta. 378 (2011) 140-147. https://doi.org/10.1016/j.ica.2011.08.047.

[10]. C.V. Sastri, D. Eswaramoorthy, L. Giribabu, and B.G. Maiya, DNA interactions of new mixed-ligand complexes of cobalt(III) and nickel(II) that incorporate modified phenanthroline ligands, J Inorg Biochem. 94 (2003) 138-145. 10.1016/s0162-0134(02)00622-0.

[11]. Z.-D. Xu, H. Liu, M. Wang, S.-L. Xiao, M. Yang, and X.-H. Bu, Manganese(II) complex of 6,7-dicycanodipyridoquinoxaline with antitumor activities: synthesis, crystal structure and binding with DNA, J. Inorg. Biochem. 92 (2002) 149-155. http://dx.doi.org/10.1016/S0162-0134(02)00569-X.

[12]. A. Sengul, H. Agac, B. Coban, and E. Eroglu, Structural studies of complex compounds of 6,6'-diacetyl-2,2'-bipyridine dioxime with copper(I/II), platinum(II), and palladium(II) metal ions, Turkish J. Chem. 35 (2011) 25-35. https://doi.org/10.3906/kim-1004-539.

[13]. W.-J. Zhang, T.-M. Ou, Y.-J. Lu, Y.-Y. Huang, W.-B. Wu, Z.-S. Huang, J.-L. Zhou, K.-Y. Wong, and L.-Q. Gu, 9-Substituted berberine derivatives as G-quadruplex stabilizing ligands in telomeric DNA, Bioorg. Med. Chem. 15 (2007) 5493-5501. https://doi.org/10.1016/j.bmc.2007.05.050.

[14]. A.G. Montalban, E.G. Sakellariou, E. Riguet, Q.J. McCubbin, A.G.M. Barrett, and B.M. Hoffman, Phenanthroline-appended porphyrazines: synthesis and conversion into solitaire Ru(II) complexes, Inorg. Chim. Acta. 317 (2001) 143-148. https://doi.org/10.1016/S0020-1693(01)00325-5.

[15]. M. Cusumano, and A. Giannetto, The interaction of mixed-ligand square-planar complexes with calf thymus DNA, J. Inorg. Biochem. 65 (1997) 137-144. https://doi.org/10.1016/S0162-0134(96)00100-6.

[16]. B. Coban, I.O. Tekin, A. Sengul, U. Yildiz, I. Kocak, and N. Sevinc, DNA studies of newly synthesized heteroleptic platinum(II) complexes $[Pt(bpy)(iip)]^{2+}$ and $[Pt(bpy)(miip)]^{2+}$, J Biol Inorg Chem 21 (2016) 163-175. https://doi.org/10.1007/s00775-015-1317-8.

[17]. B. Coban, and U. Yildiz, DNA-Binding Studies and Antitumor Evaluation of Novel Water Soluble Organic pip and hpip Analogs, Appl. Biochem. Biotech. 172 (2014) 248-262. https://doi.org/10.1007/s12010-013-0513-7.

[18]. B. Coban, U. Yildiz, and A. Sengul, Synthesis, characterization, and DNA binding of complexes $[Pt(bpy)(pip)]^{2+}$ and $[Pt(bpy)(hpip)]^{2+}$, J. Biol. Inorg. Chem. 18 (2013) 461-471. https://doi.org/10.1007/s00775-013-0991-7.

[19]. I. Kocak, U. Yildiz, B. Coban, and A. Sengul, DNA-binding studies of complex of $Pt(bpy)(pip)]^{2+}$ and $[Pt(bpy)(hpip)]^{2+}$ by electrochemical methods: development of an electrochemical DNA biosensor, J. Solid State Electrochem. 19 (2015) 2189-2197. https://doi.org/10.1007/s10008-015-2859-y.

[20]. J.B. Lepecq, and C. Paoletti, A fluorescent complex between ethidium bromide and nucleic acids: Physical—Chemical characterization, J. Mol. Biol. 27 (1967) 87-106. https://doi.org/10.1016/0022-2836(67)90353-1.

[21]. V.T. Yilmaz, C. Icsel, J. Batur, S. Aydinlik, M. Cengiz, and O. Buyukgungor, Synthesis, structures and biomolecular interactions of new silver(i) 5,5-diethylbarbiturate complexes of monophosphines targeting Gram-positive bacteria and breast cancer cells, Dalton Trans. 46 (2017) 8110-8124. https://doi.org/10.1039/c7dt01286a.

[22]. Q.-L. Zhang, J.-G. Liu, J.-Z. Liu, H. Li, Y. Yang, H. Xu, H. Chao, and L.-N. Ji, Effect of intramolecular hydrogen-bond on the DNA-binding and photocleavage properties of polypyridyl cobalt(III) complexes, Inorg. Chim. Acta 339 (2002) 34-40. http://dx.doi.org/10.1016/S0020-1693(02)00923-4.

[23]. S. Satyanarayana, J.C. Dabrowiak, and J.B. Chaires, Neither Δ- nor λ-tris(phenanthroline)ruthenium(II) binds to DNA by classical intercalation, Biochem. 31 (1992) 9319-9324. https://doi.org/10.1021/bi00154a001.

[24]. J.K. Barton, and A.L. Raphael, Photoactivated stereospecific cleavage of double-helical DNA by cobalt(III) complexes, J. Am. Chem. Soc. 106 (1984) 2466-2468. https://doi.org/10.1021/ja00320a058.

[25]. J. Borowska, M. Sierant, E. Sochacka, D. Sanna, and E. Lodyga-Chruscinska, DNA binding and cleavage studies of copper(II) complexes with 2'-deoxyadenosine modified histidine moiety, J. Biol. Inorg. Chem. 20 (2015) 989-1004. https://doi.org/10.1007/s00775-015-1282-2.

[26]. B. Coban, N. Eser, and I. Babahan, DNA binding by copper (II) complexes of semithiocarbazone containing ligands, Bulgar. Chem. Commun. 49 (2017) 908-913.

[27]. E.R. Jamieson, and S.J. Lippard, Structure, recognition, and processing of cisplatin-DNA adducts, Chem. Rev. 99 (1999) 2467-2498. https://doi.org/10.1021/cr980421n.

[28]. J. Portugal, B. Martin, A. Vaquero, N. Ferrer, S. Villamarin, and W. Priebe, Analysis of the effects of daunorubicin and WP631 on transcription, Curr. Med. Chem. 8 (2001) 1-8. https://doi.org/10.2174/0929867013373976.

[29]. C.M. Stellrecht, and L.S. Chen, Transcription Inhibition as a Therapeutic Target for Cancer, Cancers. 3 (2011) 4170-4190. https://doi.org/10.3390/cancers3044170.

[30]. F. Takusagawa, R.G. Carlson, and R.F. Weaver, Anti-leukemia selectivity in actinomycin analogues, Bioorg. Med. Chem. 9 (2001) 719-725. http://dx.doi.org/10.1016/S0968-0896(00)00293-5.

[31]. P.K.L. Fu, P.M. Bradley, and C. Turro, Stabilization of Duplex DNA Structure and Suppression of Transcription in Vitro by Bis(quinone diimine) Complexes of Rhodium(III) and Ruthenium(II), Inorg. Chem. 42 (2003) 878-884. https://doi.org/10.1021/ic020338p.

[32]. P.K.L. Fu, and C. Turro, Transcription inhibition by Rh(phi)2(phen)3+, Chem. Commun. (2001) 279-280. https://doi.org/10.1039/b007816f.

[33]. K.B. Mullis, and F.A. Faloona, Specific synthesis of DNA in vitro via a polymerase-catalyzed chain reaction, Methods Enzymol. 155 (1987) 335-350. tps://doi.org/10.1016/0076-6879(87)55023-6.
[34]. A. Bolhuis, and J.R. Aldrich-Wright, DNA as a target for antimicrobials, Bioorg. Chem. 55 (2014) 51-59. https://doi.org/10.1016/j.bioorg.2014.03.009.
[35]. I. Eryazici, C.N. Moorefield, and G.R. Newkome, Square-Planar Pd(II), Pt(II), and Au(III) Terpyridine Complexes: Their Syntheses, Physical Properties, Supramolecular Constructs, and Biomedical Activities, Chem. Rev. 108 (2008) 1834-1895. https://doi.org/10.1021/cr0781059.
[36]. S. Roy, K.D. Hagen, P.U. Maheswari, M. Lutz, A.L. Spek, J. Reedijk, and G.P. van Wezel, Phenanthroline Derivatives with Improved Selectivity as DNA-Targeting Anticancer or Antimicrobial Drugs, ChemMedChem. 3. (2008) 1427-1434. https://doi.org/10.1002/cmdc.200800097.

Figure Captions

Figure 1. Synthesis of **1** and **2**.

Figure 2. UV-Vis spectra of **1** and **2** upon the addition of CT-DNA in Tris-HCl buffer (5 mM), [Compounds] = 20 μM, [DNA]= 0-20 μM. The change in absorbance was shown by arrows. Inset: plots of [DNA]/(ε_A-ε_f) vs [DNA].

Figure 3. The change in fluorescence spectra of EtBr-DNA complex upon addition of **1** (left) and **2** (right) (0-22 and 24 μM, respectively). The arrows indicate the changes while the concentration increasing. Inset: emission-quenching curve of EtBr-DNA complex.

Figure 4. Plot of relative viscosity of CT-DNA *vs* [compound]/[DNA] in Tris buffer (5 mM Tris HCl, 25 mM NaCl) at pH 7. Showing EtBr ■, [**1**] ♦, [**2**] ▲.

Figure 5. Agarose gel electrophoresis results of pBR322 DNA after treatment with increasing concentrations of **1** (a), **2** (b). Lane 1, DNA alone; lanes 2–6, DNA was incubated for 1 h with increasing concentrations (20, 40, 60, 80, 100, 200 μM) of the compounds and (c) Lane 1, DNA alone; lane 2 DNA+H_2O_2, lanes 3–9, DNA was incubated for 1 h in the presence of H_2O_2 incubated for 1 h with increasing concentrations (20, 40, 60, 80, 100, 200, 400 μM) of **2**.

Figure 6. Transcribed mRNA on the gel electrophoresis in the presence of **1** for A) and **2** for B). Lane 1: positive control (max. amount of mRNA); lanes 2–6: increasing concentrations of (100, 200, 300, 400, and 600 μM).

Figure 7. Effect of **1** and **2** on the hybridization of oligomers (COI-F 5′-TTAAGATCCCCAGGATCATG-3′, COI-R 5′-TGCAAATACTGCACCTATTG-3′ and CytB-F 5′-TATGTACTACCATGAGGACAAATATC-3′, CytB-R 5′-ATTACACCTCCTAATTTATTAGGAAT-3′) in the PCR assay. The reactions of oligomers with various concentrations of compounds were assessed. The C lines are controls (no compounds used

and the maximum amount of DNA synthesized) and increasing concentrations of the compounds (5, 50, 500 μM) were added.

Figure 8. Cell viability ratios of HepG2 depending on concentrations of **1** and **2**.

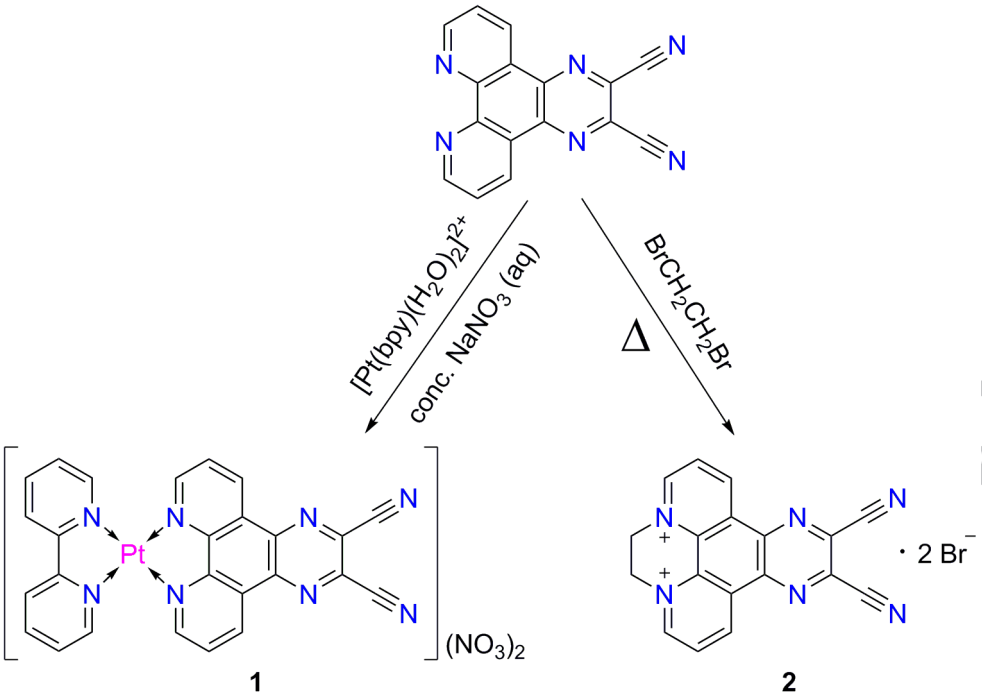

1 **2**

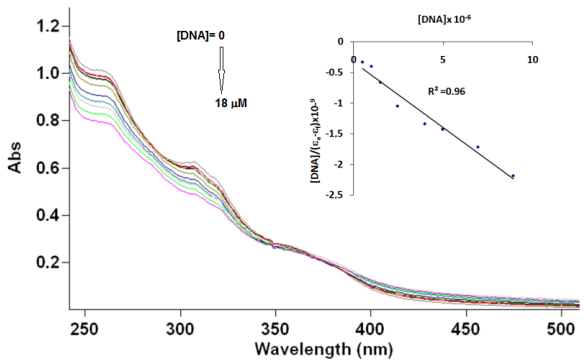

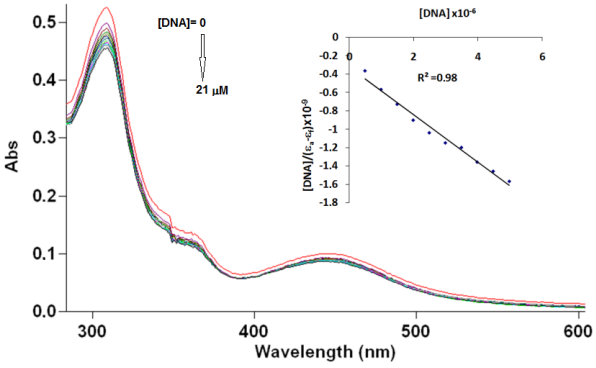

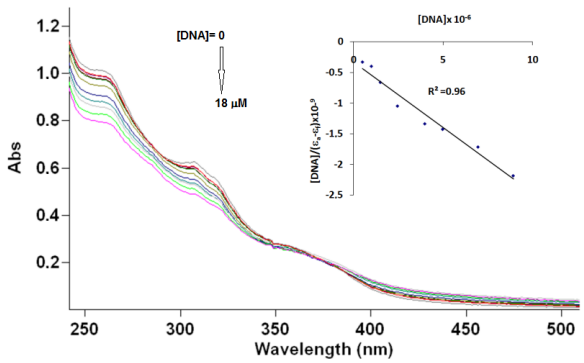

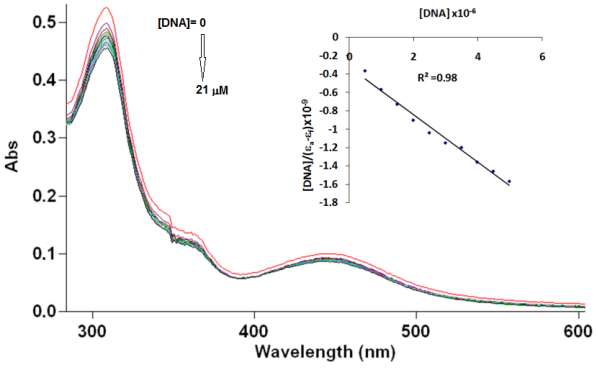

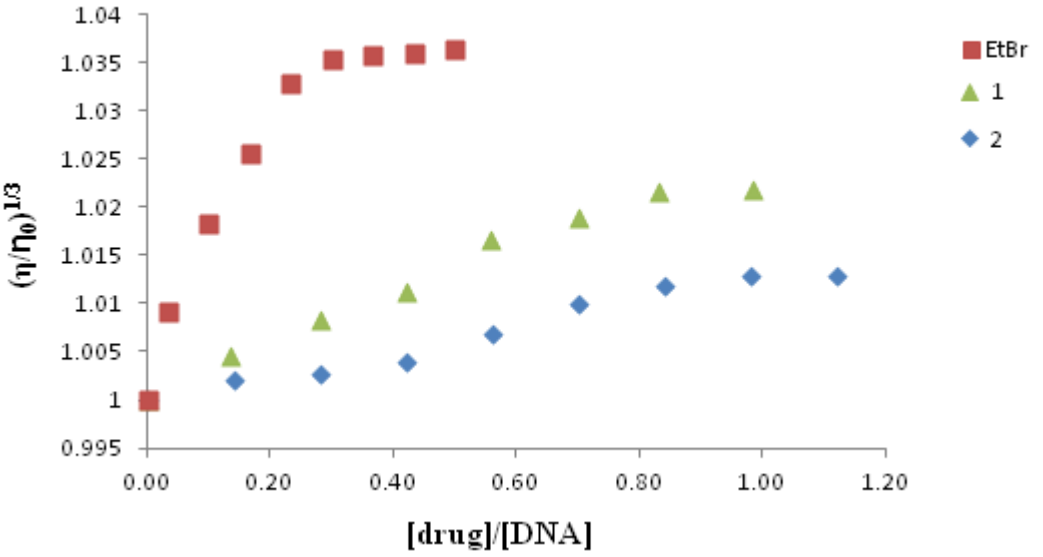

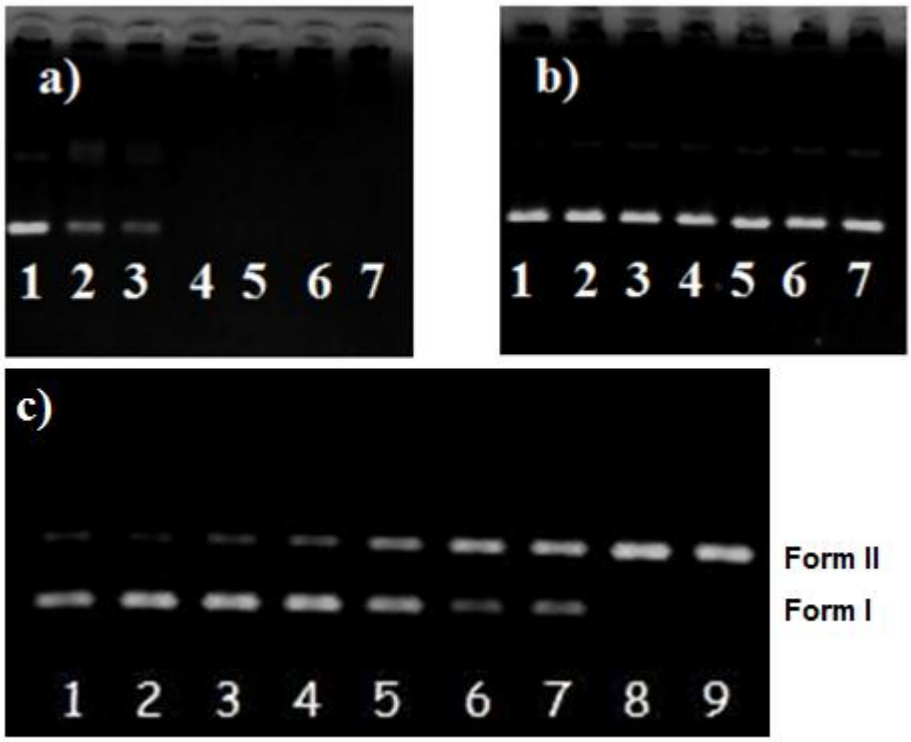

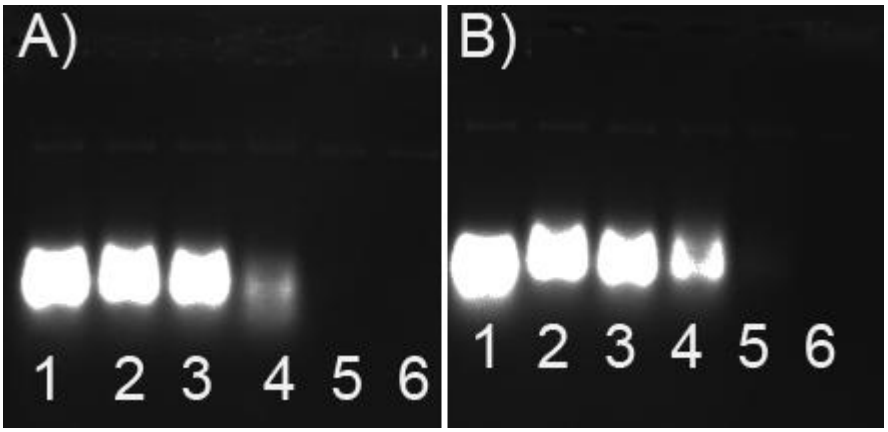

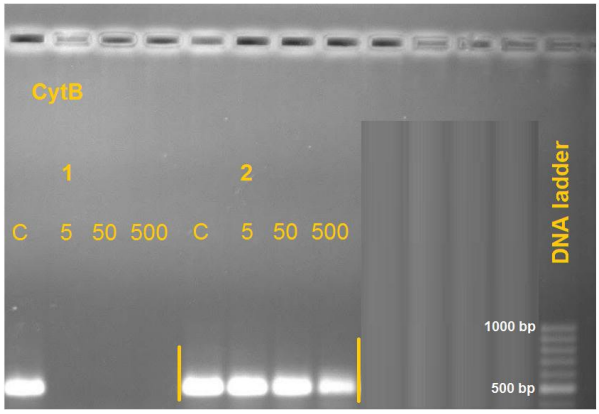

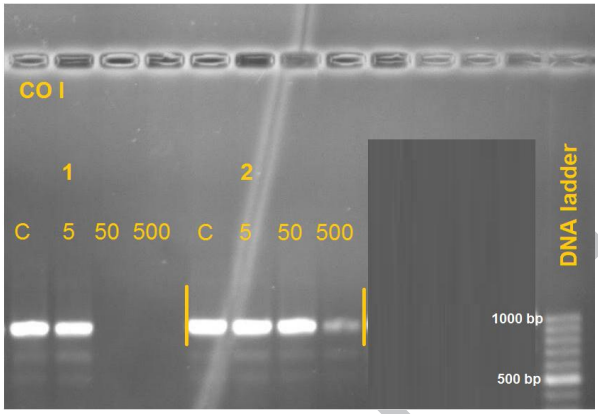

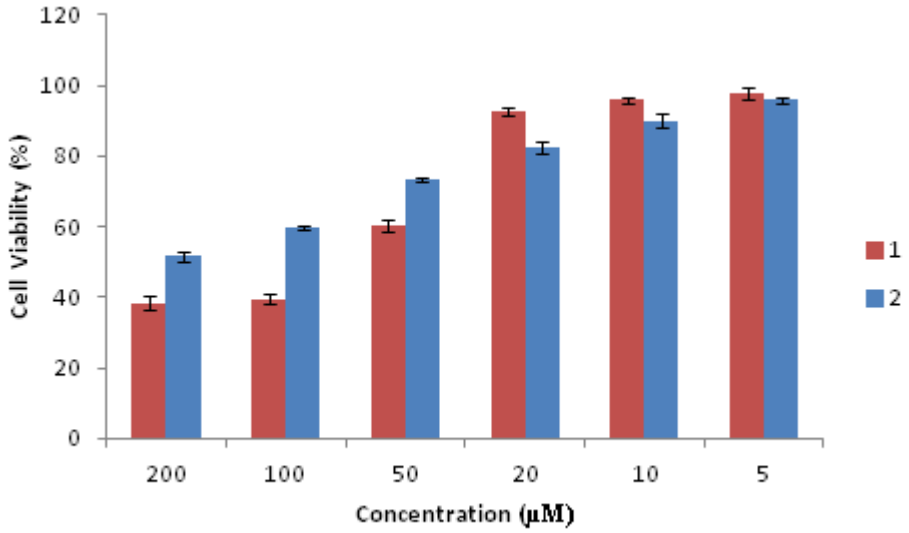

Highlights

- [Pt(bpy)(dicnq)]$(NO_3)_2$ (**1**) and quaternized dicnq (**2**) were synthesized and characterized
- **1** and **2** are both good DNA intercalators
- **1** has strong nuclease, transcriptase and Taq-polimerase inhibitory activities
- **1** is a potent antimicrobial

1 is cytotoxic against HepG2 Liver cancer cell line

Graphical abstract

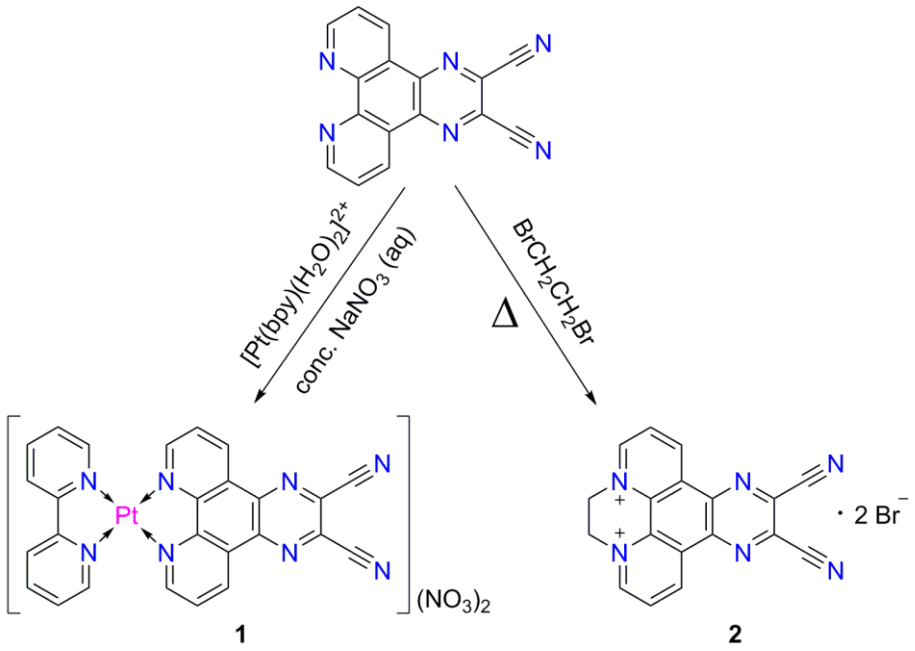

Table 3. IC_{50} values of the compounds **1** and **2** against HepG2 cell line.

Compounds	IC_{50} (μM) 48 h
1	94.75
2	159.60
Cisplatin	30.38
Ploxal-S	22.25

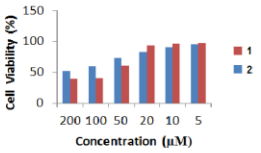

Table 4. Identified MIC values of the compounds **1** and **2**.

Compounds	*S. aureus ATCC 29213*	*E. faecalis ATCC 29212*	*E. coli ATCC 25922*	*P. aeruginosa ATCC 27853*
1	31.2	15.6	31.2	31.2
2	125	250	125	125